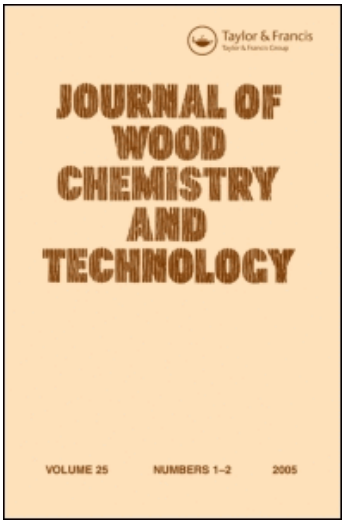

Journal of Wood Chemistry and Technology
Publication details, including instructions for authors and subscription information:
http://www.informaworld.com/smpp/title~content=t713597282

NMR Structural Characterization of *Quercus alba* (White Oak) Degraded by the Brown Rot Fungus, *Laetiporus sulphureus*

Amanda B. Koenig[a]; Rachel L. Sleighter[b]; Elodie Salmon[b]; Patrick G. Hatcher[ab]
[a] Department of Chemistry, The Ohio State University, Columbus, Ohio, USA [b] Department of Chemistry and Biochemistry, Old Dominion University, Norfolk, Virginia, USA

Online publication date: 23 February 2010

Journal of Wood Chemistry and Technology, 30: 61–85, 2010

ISSN 0277-3813 print / 1532-2319 online
DOI: 10.1080/02773810903276668

Taylor & Francis
Taylor & Francis Group

NMR Structural Characterization of *Quercus alba* (White Oak) Degraded by the Brown Rot Fungus, *Laetiporus sulphureus*

Amanda B. Koenig,[1] Rachel L. Sleighter,[2] Elodie Salmon,[2] and Patrick G. Hatcher[1,2]

[1]Department of Chemistry, The Ohio State University, Columbus, Ohio, USA
[2]Department of Chemistry and Biochemistry, Old Dominion University, Norfolk, Virginia, USA

Abstract: High resolution magic angle spinning (HRMAS) is utilized here to characterize the structure of solid lignin from *Quercus alba* (white oak) wood that has been biodegraded by the brown rot (BR) fungus *Laetiporus sulphureus*. The ground wood sample is swelled in deuterated solvent, allowing an enhanced molecular motion that is required for obtaining 2D HRMAS spectra. This technique provides for direct, non-invasive analysis of solid biodegraded lignin. Emphasis is placed on the characterization of the lignin side chains in an effort to elucidate the types of linkages connecting the various monomers. The HRMAS spectra obtained provide evidence for the presence of structures in this biodegraded lignin that have been commonly found in chemically extracted lignins and model compounds. This information supports the existence of several of the six major types of lignin linkages (β-O-4, β-5, β-1, 5-5, 4-O-5, and β-β) as well as three other structures: dibenzodioxocin, isochroman, and spirodienone.

Keywords: Cross polarization magic angle spinning; high resolution magic angle spinning, lignin degradation, lignin structure, nuclear magnetic resonance

INTRODUCTION

Lignin, found in the cell walls of vascular plants, is a major component of plant tissues. Among other functions, it provides mechanical strength to the plants and assists in water conduction.[1] Lignin is a heterogeneous solid that is insoluble in common aqueous or organic solvents and exists as a large, non-uniform biopolymer. Thus, characterization of this complex biopolymer

Address correspondence to Patrick Hatcher, Department of Chemistry and Biochemistry, Old Dominion University, Physical Sciences Building, 4402 Elkhorn Ave., Norfolk, VA 23529, USA. E-mail: phatcher@odu.edu

is rendered difficult, as lignin does not have an exact molecular structure.[2] Better characterization of its structure would not only provide insight into the chemical nature of wood, but would also lead to a deeper understanding of the composition of humic substances, as lignin is thought to be a potential precursor to soil organic matter (SOM).[3]

Lignin extracted from wood by chemical[4–6] and physical[7–10] methods has been essential for the structural characterization of lignin by solution-state single- and multi-dimensional nuclear magnetic resonance (NMR).[4–10] Lignin isolated by milling, which induces partial depolymerization, is referred to as milled wood lignin (MWL). The use of this method is preferred because it is thought to induce the least amount of structural alteration while being reasonably efficient in separating the lignin from the cellulose.[11] However, even this method of isolation causes changes in lignin structure. The ball milling procedure depolymerizes the lignin, lowering the average molecular weight. It may also cause an increase in carbonyl groups and free phenolic hydroxyl groups.[11,12]

Natural lignin cannot be completely separated from carbohydrates in wood without risking chemical alteration. Analysis of *in situ* lignin by solids NMR is difficult, as the resonance lines for carbohydrates overlap with those associated with lignin side chains.[13,14] The inherent complexity and heterogeneity of the lignin itself are responsible for analytical difficulties as well, as the lignin produces many different NMR peaks that overlap with each other.[15] To facilitate NMR peak assignments and eventual structural characterization of natural lignin, synthetic lignins, called dehydrogenation polymers (DHPs), have been synthesized and their molecular structures analyzed by modern solution-state NMR techniques. The NMR analysis of DHPs is less complicated than that of extracted lignins because DHPs contain no other wood components and the peaks in their spectra cannot be confused with peaks from carbohydrates.[16] Simplifying analysis even further, DHPs can be formed from only one type of alcohol precursor, or a combination of the three can be used to produce model polymers composed of *p*-hydroxyphenyl, guaiacyl, and syringyl units (see structures in Figure 1). Controlling the monomer composition makes it possible to determine which monomers are contributing to each NMR peak.[1,12,16] Like natural lignins, DHPs are complex, and their subunits are linked through various bond types.[1,16,17] However, as discussed by Landucci et al.,[16] the ratios of the bond types found in DHPs differ from those found in natural lignin isolates.

The characterization of lignin using 2D NMR techniques had previously been limited to solubilized extracted lignins and lignin model compounds, with the assumption that the soluble fractions are an adequate representation of the original lignin samples.[11] More recently, however, gel-state 2D NMR has also been utilized by forming a gel from ball-milled wood swelled in DMSO-d_6.[8] Further developments have been made by a recent study that has successfully acquired NMR spectra on whole cell walls without derivatization

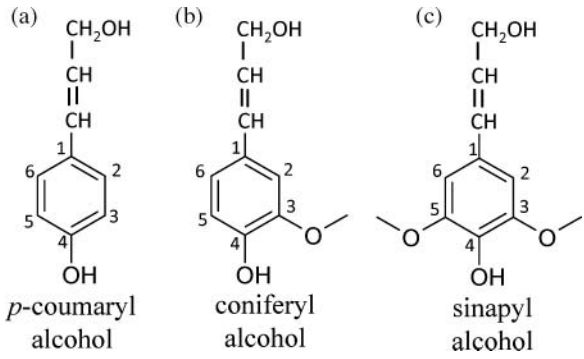

Figure 1. Lignin monomeric precursors, the monolignols a) *p*-coumeryl, b) coniferyl, and c) sinapyl alcohols, for *p*-hydroxyphenyl, guaiacyl, and syringyl units of lignin, respectively.

by dissolving ball-milled wood in the NMR tube in nondegradative solvents.[9] These approaches, however, mainly utilize traditional high resolution solution NMR and, thus, mainly examine the compounds that become partially soluble and mobile by the ball-milling and solvent-swelling process. Because extraction and ball-milling techniques can change lignin's chemical structure, natural, unfractionated, solid lignin is preferred.[14] Solid-state cross polarization magic angle spinning (CPMAS) ^{13}C NMR is the traditional method of choice for solid lignin preparations.[14,18,19] This technique has also been used to analyze the structures of DHPs and natural lignin in samples whose side chains have been labeled with ^{13}C.[14,16] Lignin side chains may have various oxidation states, displaying a combination of hydroxyl, carbonyl, and carboxyl groups, and its monomers are bonded together in irregular patterns. Furthermore, lignin can display different stereochemical arrangements, as up to two asymmetric centers on each of its side chain units are possible. The countless small variations in chemical environments for lignin produce relatively broad peaks in all NMR spectra, even in spectra of extracted lignins that have been analyzed using solution-state NMR spectrometers.

Some major shortcomings of solids NMR techniques are that peaks are not well resolved and no information on the protons is available. Fortunately, a method exists for high resolution NMR of solids that provides line widths similar to those observed in solution-state NMR. This NMR technique, high resolution magic angle spinning (HRMAS),[20–22] can provide valuable information for the study of lignin structure. HRMAS NMR allows one to obtain highly resolved 2D NMR spectra of heterogeneous, insoluble (but swelled) solid materials in natural systems.[23,24] By increasing the molecular motion of the ground lignin in the presence of a swelling solvent, as well as minimizing magnetic susceptibility effects and removing chemical shift anisotropy effects

through the use of MAS, one can obtain sufficient spectral line narrowing to employ 2D NMR techniques such as heteronuclear single quantum coherence (HSQC) and total correlation spectroscopy (TOCSY). The HSQC experiment correlates hydrogen atoms to their directly attached carbons. The TOCSY experiment correlates hydrogen atoms that are in the same spin system. The objective in using these techniques is to identify carbon and proton chemical shifts that have been previously assigned to model structures of lignin, in an effort to verify structural components in our biodegraded lignin. HRMAS has been used in recent studies to obtain 2D NMR spectra of biopolymers such as lignin, cutin, cutan, algaenan, and coal.[23–28] It is important to emphasize that this approach is only somewhat similar to previous attempts to ball-mill and solvent swell wood cell walls followed by traditional solution NMR.[8,9] However, the main difference is that the HRMAS approach purportedly observes large unsolvated macromolecular structures (that have become mobile during the swelling) as well as soluble structures. In contrast, we believe the previous studies were only observing molecules that became soluble in the solvent, as assisted by ball-milling that can rupture bonds.

We report here the use of HRMAS for the characterization of solid, untreated white oak (*Quercus alba*) lignin from wood that has been naturally biodegraded by brown rot (BR) fungi (*Laetiporus sulphureus*). While we anticipate that the BR fungi have altered the lignin somewhat, it is known that these fungi mainly attack the carbohydrates, a process which selectively enriches the wood in residual lignin.[29–31] Using advanced 2D NMR methods, that are non-invasive and capable of providing structural information on a whole, untreated sample of the biodegraded wood, will allow us to characterize the lignin at the molecular level. Our eventual goal is to establish the structural basis for tracing changes in lignin biopolymers as they become incorporated into soil organic matter (SOM).

SAMPLES AND METHODS

Origin and Preparation of Lignin

Part of a white oak tree (*Quercus alba*) that had been decomposed by the brown rot (BR) fungus *Laetiporus sulphureus* was collected in northeastern Ohio. The tree and fungus were characterized macroscopically. The sample was frozen, and the portions with the most lignin-like character (verified using solid-state CPMAS ^{13}C NMR) were ground by hand with a mortar and pestle and freeze-dried. Portions ranging in size from 53 to 106 μm were collected by dry-sieving. Elemental analysis by catalytic combustion (Thermo EA, Series 1112) indicated that the sample contains 55% carbon. The nitrogen content was below the detection limit. While the wood sample may contain some residual cellulose, it will now be referred to as BR-lignin.

Solid-State NMR

A ^{13}C NMR spectrum of the BR-lignin was obtained on a Bruker DMX 300 MHz spectrometer equipped with a solids MAS probe. The ramp CPMAS technique with two-pulse phase modulated (TPPM) decoupling, as described by Dria et al.,[32] was used. A 4 mm diameter zirconia MAS rotor with a Kel-F cap was filled with approximately 60 mg of dry sample and spun at 13 kHz at the magic angle (54.7° to the magnetic field). The experiment was carried out at 300 K using a 2 ms contact time, 1 s recycle delay time, 51200 acquisitions, and a spectral width of 30030 Hz (398 ppm). The free induction decay (FID) (1 K data) was exponentially multiplied using a line broadening of 75 Hz and zero-filled to 4096 data points. Glycine was used as an external secondary chemical shift standard (carboxyl signal at 176.03 ppm), and the recorded chemical shifts were indirectly referenced to tetramethylsilane (TMS) at 0 ppm.

HRMAS NMR

About 20 mg of lignin was swelled in DMSO-d_6 (Aldrich, 99.9% atom D) as it was packed into a 4 mm diameter zirconia MAS rotor with a Kel-F cap. A Kel-F insert was used, allowing a 50 μL volume for the sample. Highly resolved spectra of the BR-lignin were obtained using a Bruker 400 MHz spectrometer equipped with a dual channel (^1H, ^{13}C), 4 mm HRMAS probe with a single axis gradient, oriented along the magic angle. The rotor was spun at the magic angle at 10 kHz. A relaxation delay of 1 s was used for each experiment.

A ^1H-^{13}C heteronuclear single quantum coherence (HSQC) spectrum was acquired using echo-antiecho-TPPI (time proportional phase incrementation) gradient selection as well as sensitivity enhancement. In the ^1H dimension (F2), 560 scans were acquired with an acquisition time of 128 ms, each collected with 1024 data points for a spectral width of 4,006 Hz (10 ppm). In the ^{13}C dimension (F1), an acquisition time of 2.6 ms was used to collect 128 data points for a spectral width of 24,149 Hz (240 ppm). The FID in the ^{13}C dimension was zero-filled to 1024 data points. The FIDs were processed in both dimensions using a squared sine bell multiplication (QSINE) window function with a 90° phase shift.

A total correlation spectroscopy (TOCSY) spectrum was acquired with a phase sensitive pulse program that used TPPI and the MLEV-17 multiple pulse spin lock sequence. A mixing time of 100 ms was used to ensure coverage of the entire side chain coupling network. A spectral width of 5580 Hz (13.95 ppm) was used in each dimension. In the F2 dimension, 184 scans were acquired with an acquisition time of 92 ms, each with 1024 data points. In the F1 dimension, an acquisition time of 23 ms was used to collect 256 data points, which was zero-filled to 1024. The FIDs were processed in both dimensions using a QSINE window function with a 90° phase shift (i.e., cosine-squared). All of

the HRMAS spectra obtained on the 400 MHz spectrometer were calibrated using the central DMSO peak.

Procedure for the NMR Peak Assignments

Many dimers and oligomers have been synthesized and well characterized using solution-state NMR,[16,33,34] where they have become invaluable for the interpretation of NMR spectra of DHPs, and more importantly, natural lignin. The structures of particular concern have been the linkages connecting the monomeric units. While the β-O-4 linkage is the most common, several different linkages exist in the lignin biopolymer. Six major types have been established: β-O-4, β-5, β-1, 5-5, 4-O-5, and β-β.[1,35,36]

The dimers shown in Figures 2 and 3 represent six of the major types of linkages connecting lignin monomer units, as well as several types of side

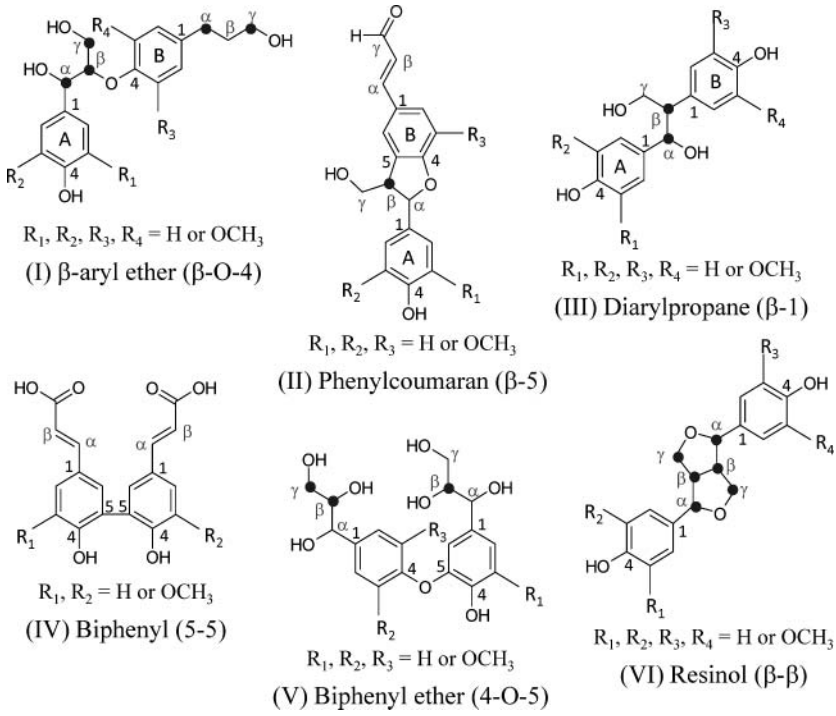

Figure 2. Dimers showing six of the major types of linkages between lignin monomers. Black dots indicate C-H data that have been assigned in HSQC spectra of this study. Lettering for α, β, and γ Hs indicate protons that have been assigned in TOCSY data of this study.

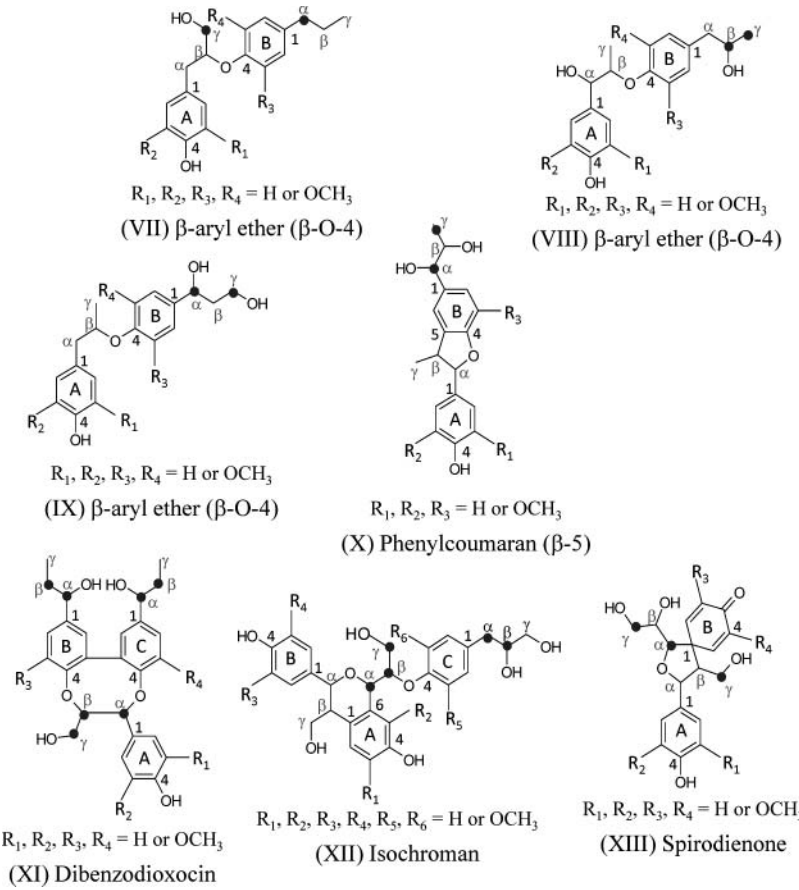

Figure 3. Dimers (VII–X) demonstrating various oxidation states of lignin side chains and additional structures (XI–XIII) that model the structures that have been demonstrated to be components of degraded lignin. Black dots indicate C—H data that have been assigned in HSQC spectra of this study. Lettering for α, β, and γ Hs indicate protons that have been assigned in TOCSY data of this study.

chains. Most of the monomers could be derived from *p*-coumaryl, coniferyl, or sinapyl alcohol monomers (i.e., *p*-hydroxyphenyl, guaiacyl, syringyl units). However, the linkages demonstrated in compounds II, IV, V, and X (β-5, 5-5, and 4-O-5), involve bonding to the C5 position and, thus, cannot involve two syringyl units.

Lignin side chain structures can exist with varying oxidation, displaying a combination of hydroxyl, carbonyl, and carboxyl groups attached at their α, β, and γ positions. Free side chains (those not connecting the monomeric units) in both saturated and unsaturated forms, containing two or three hydroxyls,

aldehyde, or carboxylic acid groups have been identified in DHPs and extracted lignins.[4] These oxidation states are demonstrated in the side chains of dimers I–VI, shown in Figure 2. However, other oxidation states are also considered in this study. As additional examples, reduced versions of the β-aryl ether dimer and phenylcoumaran dimer are shown in Figure 3. In Figures 2 and 3, black dots indicate C—H bonds that have been assigned in the HSQC data of this study, while letters for α, β, and γ Hs indicate protons that have been assigned in TOCSY data of this study. These assignments are discussed in detail in the Results sections.

In addition to the six types of linkages shown in Figure 2 others have been authenticated,[1,6,15,35,37–40] and compounds representing three different linkages are shown in Figure 3. Trimer XI is a dibenzodioxocin structure resulting from monolignol addition to a 5–5 unit. This structure has become accepted as a major lignin component.[37–39,41,42] Trimer XII demonstrates a linkage involving an aryl isochroman structure. The structure contains a β-1 linkage, and the side chain of monomer A has been shifted from the C1 position to the C6 position. Isochroman structures have been found in lignin isolated from pine wood by a degradation procedure called the DFRC (derivatization followed by reductive cleavage) method. In addition, small peaks representing the isochroman structure have been found in 2D NMR spectra of acetylated pine MWL.[15,40] The spirodienone structure found in dimer XIII was discussed by Brunow et al.[39] The authors proposed that the β-1 linkage demonstrated in dimer III may not be present in natural lignin, but instead be formed from the acidolysis of lignin (commonly used to cleave lignin monomers). The presence of the spirodienone structure in natural lignins has recently been demonstrated with NMR.[6,43]

The compounds illustrated in these figures are utilized as representative model structures found in natural lignin, and as such, are referenced in interpreting the NMR spectra in this study. However, because the BR-lignin sample was analyzed without extraction or processing, it is expected to be comprised of large polymeric structures; dimers and trimers are not expected to be present as such in great abundance. The structures are only used as models for demonstrating the types of structural entities present and bonding interactions one could observe between various monomer types.

Relatively broad lineshapes are found in the HSQC and TOCSY spectra of the complex lignin biopolymer of *Quercus alba* degraded by BR fungi, compared to the narrower lineshapes observed for dimers and trimers.[4,33] Also, the small model compounds that are reported in a database[33] were each analyzed separately so there were no overlapping peaks from slightly different monomers or oligomers. Half of the ^{1}H chemical shifts for the model compounds provided by Ralph et al.[33] were determined in acetone or chloroform, not DMSO. All but one of the spectra used to determine the ^{13}C chemical shifts were acquired in DMSO. This, combined with the heterogeneity of the natural lignin, provided some difficulty in making accurate structural assignments for the Hs and Cs of

each peak in the biodegraded BR-lignin spectra. The TOCSY peaks are very closely spaced, and some are overlapping, especially the peaks found between 3 and 5 ppm. In some instances, the difference between the chemical shifts of two peaks is no larger than the difference between the chemical shifts of two peaks produced from identical compounds analyzed in two different solvents. Many of the peaks in the HSQC and TOCSY spectra of the biodegraded BR-lignin have been assigned to several different types of side chains in this study. It is possible that each of these cross peaks has been produced from many different types of Hs and Cs and are not unique to one assigned structure. Because the BR-lignin in this study was not modified by acetylation, a method commonly used to differentiate ambiguous chemical shifts,[16,33] we cannot determine with certainty that the linkages found in compounds XI, XII, and XIII are present. The unacetylated shifts are too easily confused with the chemical shifts of more established side chains.

The vast majority of the chemical shift assignments are based on the assignments of model compounds reported by the United States Forest Products Laboratory and Dairy Forage Research Center.[33] Peaks in the HSQC and TOCSY spectra were assigned to specific structural entities if the ^{1}H dimension chemical shifts matched to within 0.3 ppm of the model compound chemical shifts and the ^{13}C dimension shifts were within 2.2 ppm. The lineshapes were broader in the ^{13}C dimension, so a greater mismatch was allowed. An exception was made for the α carbon of compound VII, monomer B. The ^{13}C chemical shift in the HSQC spectrum was off by 2.6 ppm, but we attribute this to the proximity to the DMSO solvent peak which is the central peak of the cluster. While the peak assignments made for these compounds should be considered as tentative, they are a reasonable approximation for the types of structures shown in Figures 2 and 3.

RESULTS AND DISCUSSION

Structural Assignments

Identification of Structural Moieties by CPMAS ^{13}C NMR

The CPMAS ^{13}C NMR spectrum of the BR-lignin is shown in Figure 4. The spectrum is characteristic of hardwood that has been degraded by brown rot (BR) fungi.[29,30,44] Peaks representing both guaiacyl and syringyl units (see Figure 1) are present, verifying that the sample originates from an angiosperm wood. The peak at 153 ppm is derived from C3 and C5 of etherified syringyl units (e.g., syringyl units bonded through β-O-4 linkages) as well as C4 of etherified guaiacyl units (see Figures 1 and 2 for the carbon numbering scheme for lignin). The peak at 147 ppm arises from C3 and C4 of guaiacyl units as well as C3 and C5 of syringyl units from non-etherified lignin. In general,

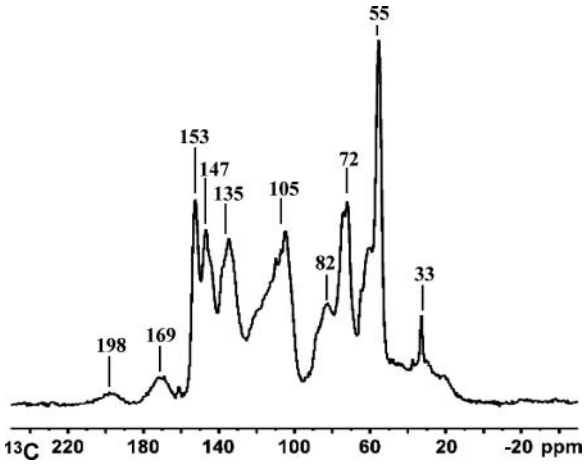

Figure 4. CPMAS ^{13}C NMR spectrum of brown-rotted (BR) lignin.

however, the peak at 153 ppm is usually assigned to syringyl lignin, while the peak at 147 is assigned to guaiacyl lignin. The broad peak at 135 ppm arises from C1 in all lignin monomeric units as well as C4 in syringyl units.[13,29,45] Most of the carbohydrates have been degraded, as indicated by the relatively low intensity of the peak at 72 ppm, which typical dominates the spectrum of fresh wood.[46] The signals at 72 and 82 ppm can be assigned to the carbons of lignin side chains. The peak at 105 ppm is assigned to C2 and C6 in syringyl lignin for this sample. Peaks at 198 ppm and 169 ppm are representative of carbonyl and carboxyl carbons, respectively, and can indicate lignin oxidation. The most intense peak in the spectrum at 55 ppm is attributed to the methoxyl carbons in lignin. Finally, the alkyl signals at 33 ppm and in the broad range from 50 to 0 ppm could be an indication of residual BR fungal lipids.[13,29,45,47]

Identification of Structural Moieties by ^{1}H-^{13}C HSQC HRMAS

The ^{1}H-^{13}C HSQC HRMAS NMR spectrum, obtained after swelling the solid, BR-lignin sample in DMSO-d_6, is shown in Figure 5. The horizontal axis displays the ^{1}H chemical shifts and the vertical axis represents the ^{13}C chemical shifts. Cross peaks are only observed for carbons that have directly attached protons. The peaks that appear between 6 and 8 ppm in the ^{1}H dimension and between 100 and 120 ppm in the ^{13}C dimension derive from Hs and Cs on the aromatic rings of lignin. An enlarged plot of this region is shown in Figure 6. The aromatic ring Cs that are substituted with hydroxyl or methoxyl groups do not appear because they are not bonded directly to Hs. The aromatic rings of guaiacyl and syringyl units all contribute to these broad peaks, and the assignments are indicated in Figure 6. The signals assigned to aromatic syringyl

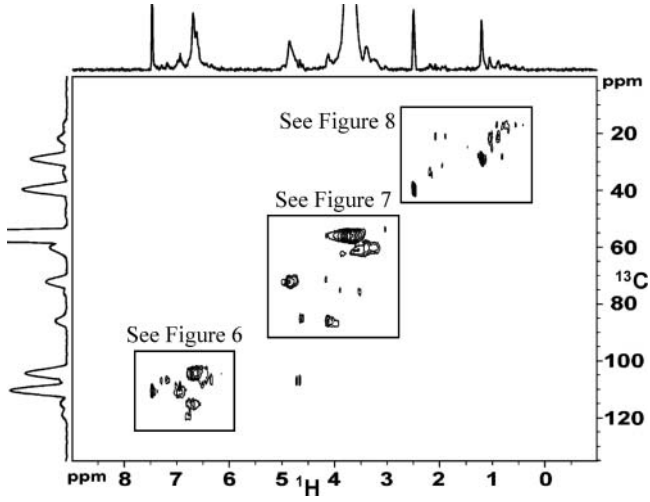

Figure 5. ^{1}H-^{13}C HSQC HRMAS NMR spectrum of brown-rotted (BR) lignin swelled in DMSO-d_6.

Cs and Hs appear more upfield (lower ppm), while aromatic peaks from guaiacyl and *p*-hydroxyphenyl structures are at higher ppm. Due to the broadness of the various peaks and the vast possibilities for bonding interactions, it is only possible to make general assignments to units derived for the types of lignin

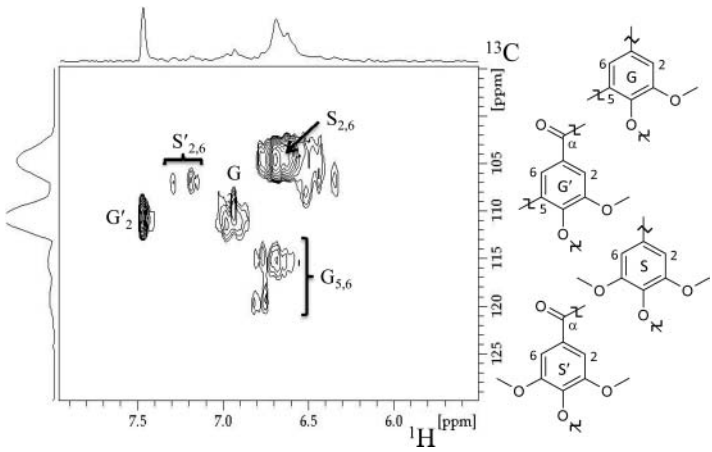

Figure 6. Expanded plot from the ^{1}H-^{13}C HSQC HRMAS NMR spectrum of brown-rotted (BR) lignin shown in Figure 5. "S" refers to syringyl units and "G" to guaiacyl units. Assignment abbreviations refer to the structures shown to the right of the figure.

monomers. The upfield peaks labeled $S_{2,6}$ are assigned to C2 and C6 of a syringyl unit. The relatively weak peaks labeled $S_{2,6}'$ correspond to C2 and C6 of syringyl units substituted with carbonyl or carboxyl functional groups on C1. The peak marked G_2 is assigned to C2 of guaiacyl units, while the two broad peaks labeled $G_{5,6}$ is assigned to C5 and C6 of guaiacyl or *p*-hydroxyphenyl units. It is likely that guaiacyl units are the main contributors to these peaks, as typical peaks representing C2 and C6 from *p*-hydroxyphenyl units are not present between 7.1–7.6 ppm in the ^{1}H dimension and 126–131 ppm in the ^{13}C dimension and *p*-hydroxyphenyl units are not large components of angiosperms.[33,48]

In Figure 5, the very broad peak found at 3.74 ppm in the ^{1}H dimension and 56.40 ppm in the ^{13}C dimension is derived from the methoxyl groups attached to the lignin aromatic rings. Again, a wide range of chemical environments produce broad spectral lineshapes in both dimensions. At least two types of lignin side chain carbons and hydrogens also contribute to this peak, and these are indicated in Figure 7, which shows an expanded plot of this region. The cross peaks identified within the spectrum are assigned to the lignin structures shown in Figures 2 and 3 and will be discussed in a later section.

Many of the peaks in Figure 5 detected between 0 and 2.6 ppm in the ^{1}H dimension and between 0 and 50 ppm in the ^{13}C dimension are probably from lipids associated with the BR fungus. However, specific assignments are not possible at this time due to the uncertainty of the types of structures present

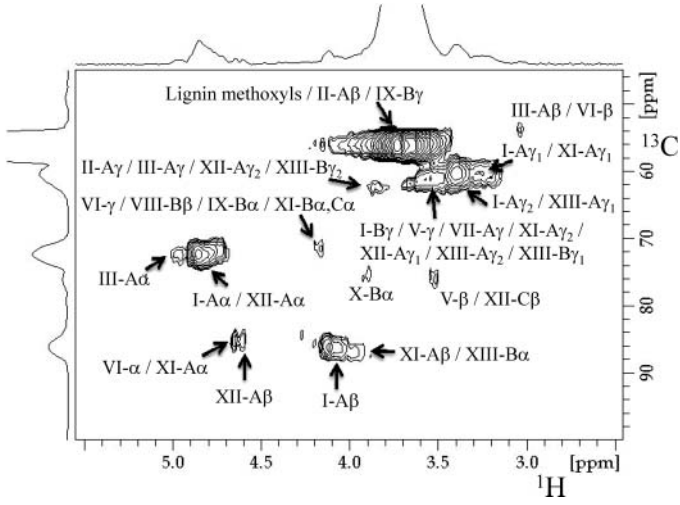

Figure 7. Expanded plot from the ^{1}H-^{13}C HSQC HRMAS NMR spectrum of brown-rotted (BR) lignin shown in Figure 5. The symbols refer to lignin structures shown in Figures 2 and 3 and summarized in Table 1.

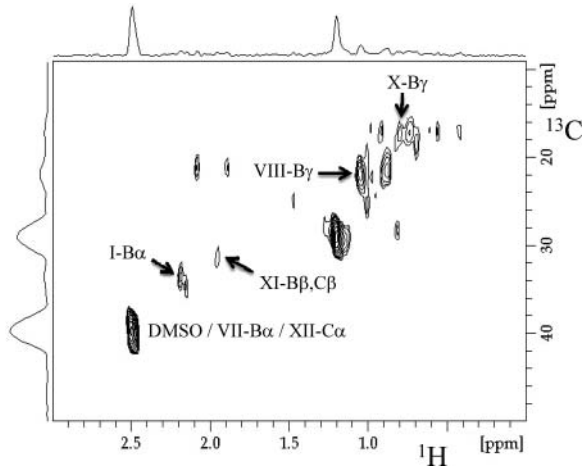

Figure 8. Expanded plot from the ^{1}H-^{13}C HSQC HRMAS NMR spectrum of brown-rotted (BR) lignin shown in Figure 5. The symbols refer to lignin structures shown in Figures 2 and 3 and summarized in Table 1.

from the fungi. Cross peaks for lignin side chain structures are also possible in this region, and these are indicated in an expanded plot shown in Figure 8. The peak at 2.50, 39.52 ppm (^{1}H, ^{13}C dimension) is assigned to the central DMSO solvent peak, but at least two types of lignin alpha Cs and Hs overlap with this strong solvent peak.

The majority of the non-aromatic peaks in the HSQC spectrum (see Figures 5, 7, and 8) can be assigned to lignin side chains. The peaks in the enlarged plots of the HSQC spectrum (Figures 7 and 8) are each labeled and correspond to a symbol that indicates which dimer or trimer (I–XIII), monomeric unit (A, B, or C), and specific carbon and hydrogen (α, β, or γ) models the peak to which the structure can reasonably be assigned (see structures in Figures 2–3). The chemical shifts assigned to the side chains of structures I–XIII are summarized in Table 1.

Identification of Structural Moieties by ^{1}H-^{1}H TOCSY HRMAS

The TOCSY HRMAS NMR spectrum of the solid BR-lignin swelled in DMSO-d_6 is shown in Figure 9. Hs that communicate through spin coupling across multiple bonds (i.e., J-coupling) show off-diagonal cross peaks that identify the chemical shifts of the communicating partners. Thus, one can establish the proton coupling network in molecules, a valuable tool for establishing the overall structure of organic compounds. For a complicated structural entity such as lignin, one might expect multiple chemical shift environments to broaden the spectra and render them less useful in this regard. However, the spectrum

Table 1. Chemical shifts of the peaks labeled in the expanded plots of the ^{1}H-^{13}C HSQC HRMAS NMR spectrum of BR-lignin swelled in DMSO-d_6 (Figures 7 and 8), corresponding to structures shown in Figures 2 and 3

Carbon Label	Symbol of the Structure	^{1}H Chemical Shift (ppm)	^{13}C Chemical Shift (ppm)
4a	lignin methoxyls, II-Aβ, IX-Bγ	3.74	56.40
4b	III-Aβ, VI-β	3.03	54.06
4c	I-Aγ_1, XI-Aγ_1	3.23	60.62
4d	I-Aγ_2, XIII-Aγ_1	3.39	60.15
4e	I-Bγ, V-γ, VII-Aγ, XI-Aγ_2, XII-Aγ_1 XIII-Aγ_2, XIII-Bγ_1	3.57	61.56
4f	II-Aγ, III-Aγ, XII-Aγ_2, XIII-Bγ_2	3.88	62.26
4g	VI-γ, VIII-Bβ, IX-Bα, XI-Bα, XI-Cα	4.17	71.64
4h	III-Aα	5.01	72.34
4i	I-Aα, XII-Aα	4.86	72.58
4j	X-Bα	3.91	75.39
4k	V-β, XII-Cβ	3.52	75.62
4l	VI-α, XI-Aα	4.66	85.47
4m	XII-Aβ	4.62	85.47
4n	I-Aβ	4.12	86.41
4o	XI-Aβ, XIII-Bα	3.94	87.11
5a	X-Bγ	0.80	17.48
5b	VIII-Bγ	1.04	22.17
5c	XI-Bβ, XI-Cβ	1.95	31.55
5d	I-Bα	2.20	32.96
5e	DMSO, VII-Bα, XII-Cα	2.50	39.52
5f	methyl group bonded to olefinic group	1.9–2.1	21.0

shown in Figure 9 indicates well-resolved cross peaks that provide sufficient information to allow assignments to be made to specific lignin structures shown in Figures 2 and 3 and to other components of the sample.

The peaks that correlate Hs with chemical shifts between 4.5 and 5.5 ppm to Hs with chemical shifts between 0 and 2.6 ppm could be assigned to lipids from the BR fungus (see expanded plot in Figure 10). These peaks (especially the $J_{olefinic}$ cluster centered at 5.4, 1.9 ppm) are characteristic of Hs attached to olefinic carbons correlated with Hs attached to alkane carbons. The peaks that correlate Hs, found between 0 and 2.6 ppm, to other Hs, between 0 and 2.6 ppm, could also represent lipids from BR fungi (see expanded plot in Figure 11). They could be assigned to the saturated portions of the lipid chains. The numbered cross peaks in the enlarged spectra are assigned to the lignin structures shown in Figures 2 and 3 and will be discussed in the next section.

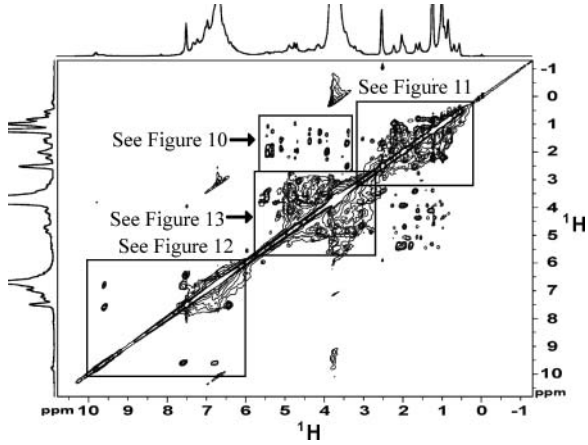

Figure 9. TOCSY HRMAS NMR spectrum of brown-rotted (BR) lignin swelled in DMSO-d_6.

While there is significant aromatic H intensity in the TOCSY spectrum in the region of 6.2–7.6 ppm, there are few resolved cross peaks that can be assigned to aromatic Hs within a single spin system (see the expanded plot in Figure 12). This is because most aromatic Hs on lignin substructures are not

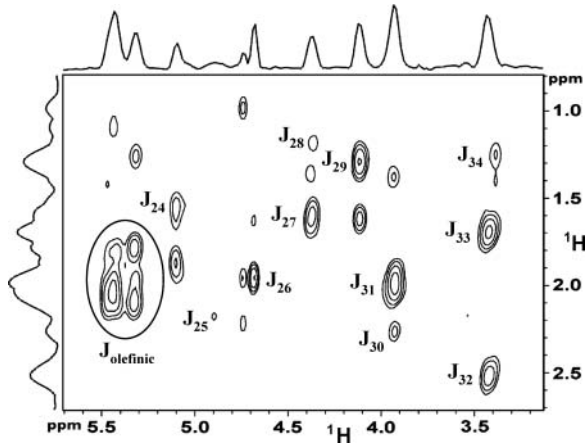

Figure 10. Expanded plot from the TOCSY HRMAS NMR spectrum of brown-rotted (BR) lignin shown in Figure 9. The numbered peaks are listed in Table 2 and are assigned to specific lignin structures shown in Figures 2 and 3. The peaks that correlate Hs with chemical shifts between 4.5 and 5.5 ppm to Hs with chemical shifts between 0 and 2.6 ppm could also be assigned to lipids from the brown rot fungus.

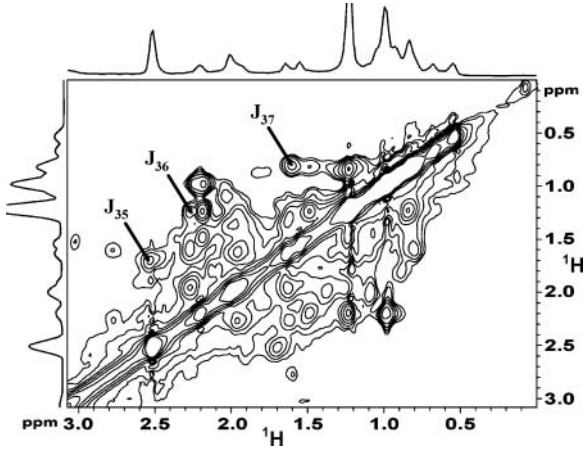

Figure 11. Expanded plot of the alkane region of the TOCSY HRMAS NMR spectrum of brown-rotted (BR) lignin shown in Figure 9. The numbered peaks are listed in Table 2 and are assigned to specific lignin structures shown in Figures 2 and 3. The majority of the remaining peaks are likely to be from fungal lipids.

communicating within a connected spin system, and the Hs that are communicating appear at very similar chemical shifts. Thus, the broad cross peak region is typical of what one would expect from most lignin aromatic Hs. Peak J_3 in the spectrum, the only clearly resolved aromatic cross peak, is assigned to C5

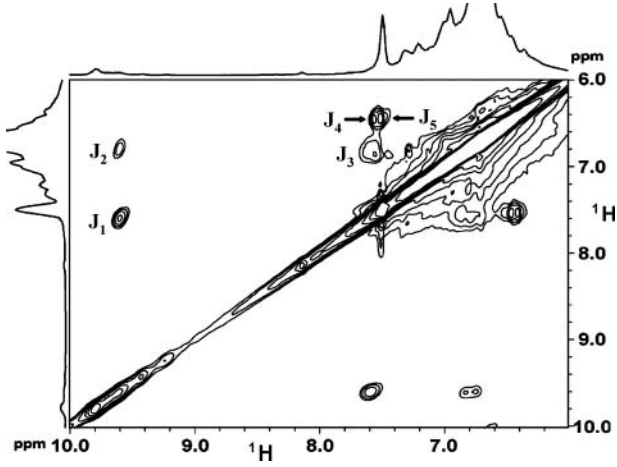

Figure 12. Expanded plot of the aromatic and aldehyde regions of the TOCSY HRMAS NMR spectrum of brown-rotted (BR) lignin shown in Figure 9. The numbered peaks are listed in Table 2 and are assigned to specific lignin structures shown in Figures 2 and 3.

Hs coupled to C6 Hs on the aromatic rings of *p*-hydroxyphenyl and guaiacyl lignin structures. This peak is likely derived from guaiacyl aromatic Hs, since *p*-hydroxyphenyl units are not main components of angiosperms. There are no coupled hydrogens on the aromatic rings of syringyl units so there are no TOCSY peaks for syringyl aromatic rings. The TOCSY spectrum clearly shows the presence of cross peaks for aldehyde Hs in the region of 9–10 ppm. Peaks J_1 and J_2 are characteristic of lignin side chain olefins (α, β-unsaturated) bonded to aldehydes as demonstrated in compound II. In addition to correlating with the aldehyde, they correlate with each other (peak J_3).

The dense group of peaks that correlate Hs with chemical shifts between 3 and 5 ppm to other Hs between 3 and 5 ppm, shown in the expanded region of the TOCSY spectrum in Figure 13, represent the diverse group of lignin side chains. Most of these peaks, as well as many of the peaks that appear elsewhere in the TOCSY spectrum (see the expanded plots in Figures 10 and 13), can be attributed to the various lignin side chains found in compounds I through XIII. The chemical shifts of the peaks that could be formed from the side chain Hs of dimers I through VI, as well as those that could emerge as a result of the alternative oxidation states (up to three hydroxyl, carbonyl, or carboxyl functional groups substituted on the side chain) demonstrated in dimers VII through X, are listed in Table 2. Many of the TOCSY peaks can also be assigned to the free side chains and interlinked side chains in compounds XI, XII, and XIII, and their chemical shifts are also listed in Table 2. The J-coupling peaks in the enlarged TOCSY spectra are labeled with numbers. Those numbers are matched with the peaks' chemical shifts in Table 2. Also

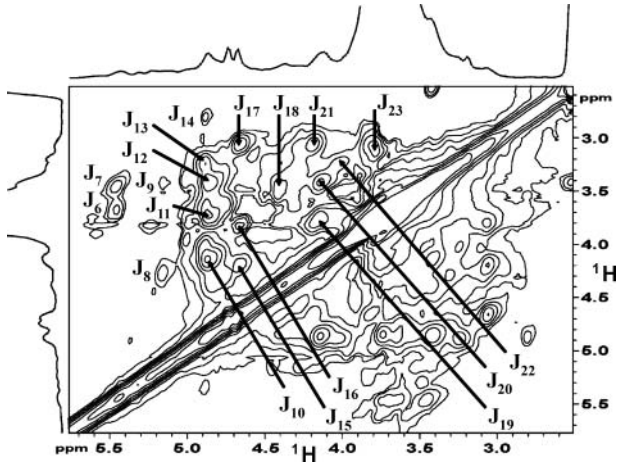

Figure 13. Expanded plot from the TOCSY HRMAS NMR spectrum of brown-rotted (BR) lignin shown in Figure 9. The numbered peaks are listed in Table 2 and are assigned to specific lignin structures shown in Figures 2 and 3.

Table 2. Chemical shifts of the peaks labeled in the expanded plots of the TOCSY HRMAS NMR spectrum of BR-lignin swelled in DMSO-d_6 (Figures 10–13), corresponding to structures shown in Figures 2 and 3

J coupling	Dimer Symbol	^{1}H Chemical Shifts (ppm)	
J^1	II-Bγ, II-Bα	9.59	7.59
J_2	II-Bγ, II-Bβ	9.59	6.80
J_3	II-Bα, II-Bβ; lignin aromatic rings	7.56	6.84
J_4	IV-α, IV-β	7.54	6.44
J_5	IV-α, IV-β	7.50	6.42
J_6	II-Aα, II-Aγ	5.44	3.64
J_7	II-Aα, II-Aβ	5.44	3.44
J_8	VIII-Aα, VIII-Aβ	5.13	4.25
J_9	X-Aα, X-Aβ	5.13	3.44
J_{10}	I-Aα, I-Aβ	4.84	4.12
J_{11}	I-Aα, I-Aγ_2; III-Aα, III-Aγ; XI-Aα, XI-AB; XI-Aα, XI-Aγ_2; XIII-Aα, XIII-Aγ_2	4.83	3.71
J_{12}	I-Aα, I-Aγ_1 ; XIII-Aα, XIII-Aγ_1	4.83	3.40
J_{13}	XI-Aα, XI-Aγ_1	4.86	3.23
J_{14}	III-Aα, III-Aβ	4.86	2.78
J_{15}	VI-α, VI-γ ; XII-Aα, XII-Aβ	4.64	4.16
J_{16}	IX-Bα, IX-Bγ; XII-Aα, XII-Aγ	4.64	3.81
J_{17}	VI-α, VI-β	4.64	3.04
J_{18}	V-α, V-β; V-α, V-γ; X-Bα, X-Bβ; XII-Bα, XII-Bβ	4.38	3.46
J_{19}	I-Aβ, I-Aγ_2 ; VII-Aβ, VII-Aγ; XII-Aα, XII-Aγ; XIII-Bα, XIII-Bβ ; XIII-Bγ_2, XIII-Bβ; XIII-Bα, XIII-Bγ_1	4.13	3.74
J_{20}	I-Aβ, I-Aγ_1 ; XII-Bγ, XII-Bβ	4.12	3.40
J_{21}	VI-γ, VI-β; VII-Aβ, VII-Aα; IX-Aβ, IX-Aα	4.17	3.03
J_{22}	XI-Aβ, XI-Aγ_1	4.00	3.21
J_{23}	VII-Aγ, VII-Aα	3.79	3.07
J_{24}	VIII-Aα, VIII-Aγ; X-Aα, X-Aγ	5.08	1.56
J_{25}	XIII-Aα, XIII-Aβ	4.89	2.18
J_{26}	IX-Bα, IX-Bβ	4.67	1.95
J_{27}	VII-Aβ, VII-Aγ; XI-Bα/Cα, XI-Bβ/Cβ	4.36	1.60
J_{28}	X-Bα, X-Bγ	4.35	1.18
J_{29}	IX-Aα, IX-Aγ	4.11	1.29
J_{30}	XIII-Aγ, XIII-Aβ	3.93	2.26
J_{31}	IX-Bα, IX-Bβ	3.92	1.99
J_{32}	I-Bγ, I-Bα; VIII-Bβ, VIII-Bα	3.41	2.52
J_{33}	I-Bγ, I-Bβ; X-Aβ, X-Aγ	3.41	1.69
J_{34}	VIII-Bβ, VIII-Bγ	3.38	1.25
J_{35}	I-Bα, I-Bβ; VII-Bα, VII-Bβ	2.51	1.68
J_{36}	VIII-Bα, VIII-Bγ	2.26	1.24
J_{37}	VII-Bβ, VII-Bγ; XI-Bβ/Cβ, XI-Bγ/Cγ	1.59	0.79
$J_{olefinic}$	Hs on olefinic Cs coupled to Hs on alkane Cs	5.4	1.9

listed in the table are symbols indicating the specific hydrogens (α, β, or γ) found in each monomeric unit (A, B, or C) from each dimer or trimer (I-XIII) that could reasonably have caused the presence of the numbered TOCSY peaks.

Identification of the Different Types of Linkages and Side Chains

Despite the drawbacks, the information obtained from the HSQC and TOCSY spectra of natural, biodegraded BR-lignin is very valuable. Through comparisons to lignin model compounds, the presence of well-established linkages as well as the occurrence of side chains variously substituted by oxygen functionalities have been supported in a sample examined non-invasively. The most common linkage, the β-O-4 linkage, is demonstrated in compound I. The side chain of monomer A is involved in the linkage. As would be expected, the HSQC peaks representing the α, β, and γ carbons and Hs of monomer A are very intense, verifying that a large amount of the β-O-4 linkage remains in the biodegraded BR-lignin sample (Figure 7). The Hs associated with this structure are also well represented in the TOCSY spectrum (Figure 13). There is also evidence for the free side chain of monomer B in both the HSQC and TOCSY spectra (Figures 7, 8, 10, and 11), although there is no peak corresponding to I-Bβ in the HSQC spectrum.

The β-5 linkage of phenylcoumaran structures is shown in compound II. The evidence for this structure in the HSQC spectrum is difficult to confirm, because the cross peak representing the β C/H from monomer A overlaps with the broad methoxyl peak at 3.74 ppm in the ^{1}H dimension and 56.40 in the ^{13}C dimension (Figure 7). Also, there is no peak corresponding to the α C/H from monomer A, and the γ peak is small and can be assigned to several other lignin side chain structures (Figure 7). However, peaks J_6 and J_7 in the TOCSY spectrum provide strong evidence for the phenylcoumaran linkage and cannot be assigned to any of the other lignin models (Figure 13). The peak coordinating the β and γ Hs of monomer A may or may not be present, as it would appear in an unresolved area of the spectrum. The free side chain of monomer B in compound II consists of an aldehyde bonded to an alkene. While there is no evidence for this structure in the HSQC spectrum, mainly because an insufficient spectral width was employed in data collection, its peaks are very clearly present in the TOCSY spectrum, denoted by peaks J_1 and J_2 which could not be assigned to structures other than side chain α, β-unsaturated aldehydes (Figure 12).

Compound III represents structures linked by the β-1 linkage, which had been previously questioned as a reasonable component of native lignin.[35,39] HSQC peaks can be assigned to the α, β, and γ positions of compound III (Figure 7). In the TOCSY spectrum, peak J_{14} could correlate the α and β Hs, and peak J_{11} could correlate the α and γ Hs (Figure 13). However, there is no peak correlating the β and γ Hs. Therefore, the presence of the β-1 linkage cannot be completely verified in this biodegraded wood sample. In a recent

publication,[6] structures linked by the β-1 bond type have been described as spirodienones and diarylpropanes. If these structures exist in our sample, then we cannot support the concept that they are major components because not all cross peaks for the side chain protons are observed.

The 5-5 biphenyl linkage shown in compound IV cannot be analyzed with these techniques, as the linkage does not involve the side chains. Instead, the side chains are unlinked and consist of γ carboxylic acids bonded to α, β alkenes. There is no evidence for these side chains in the HSQC spectrum, but there is clear evidence in the TOCSY spectrum. TOCSY peaks J_4 and J_5 could both represent the correlations between the α and β Hs (Figure 12).

The 4-O-5 linkage shown in compound V does not involve the side chains either and cannot be verified. However, peaks can be assigned to the hydroxylated side chains, which could exist as structural units attached to many of the possible aromatic lignin subunits. In the HSQC spectrum, a small peak could be attributed to the β position (Figure 7). A large peak could be assigned to the γ position; however, the same peak could be assigned to many other types of γ carbons and Hs. An HSQC peak representing the α position is not present. In the TOCSY spectrum, peak J_{18} could correlate the α and β hydrogens of compound V (Figure 13). However, the peak is assignable to other Hs as well (see Table 2). Compound VI is representative of the β-β resinol structure. Small HSQC peaks can be assigned to the α, β, and γ carbons and Hs of this compound (Figure 7). Peaks J_{15}, J_{17}, and J_{21} in the TOCSY spectrum are additional evidence that the α, β, and γ hydrogens are present, and peak J_{17} is unique to this structure (Figure 13).

There is evidence that some of the side chains in the biodegraded lignin are partially hydroxylated. Examples of structures such as these are represented by compounds VII, VIII, IX, and X (as well as the free side chains of dimers I, XI, and XII). In the HSQC spectrum, there are peaks that could be assigned to Aγ, Bα, and Bβ of compound VII (Figures 7 and 8); Bβ and Bγ of compound VIII (Figures 7 and 8); Bα and Bγ of compound IX (Figure 7); and Bα and Bγ of compound X (Figures 7 and 8). While the HSQC data only weakly supports the presence of these side chains, the TOCSY spectrum is more definitive in showing their presence. With the exception of the α,β-dihydroxylated side chain of monomer B in compound X, peaks correlating each of the Hs in the side chains of compound VII (Figures 1 and 13), compound VIII (Figure 10, 11, and 13), compound IX (Figures 10 and 13), and compound X (Figures 10 and 13) are found in the TOCSY spectrum.

Compound XI demonstrates the dibenzodioxocin structure as well as another substitution state (α-monohydroxylated) for free side chains. The trialkoxyl side chain of monomer A is involved in the dibenzodioxocin structure. Peaks in the HSQC spectrum can be assigned to Aα, Aβ, Aγ_1, and Aγ_2 of this structure (Figure 7). In the TOCSY spectrum, peaks J_{11}, J_{13}, and J_{22} correlate the α, β, and γ hydrogens of monomer A, and peaks J_{13} and J_{22} cannot be assigned to other types of lignin structures (Figure 13). Free side chains, in α-monohydroxylated states, are attached to monomers B and C. Peaks in the

HSQC spectrum could be assigned to the α and β positions of monomers B and C (Figures 7 and 8), and peaks in the TOCSY spectrum correlate the α, β, and γ hydrogens of these monomers (Figures 10, 11, and 13).

The isochroman structure is represented by compound XII, and the side chains of monomers A and B are involved in this linkage. As mentioned previously, the side chain of monomer A has been shifted from the C1 position to the C6 position. The side chain of monomer C demonstrates another potential free side chain β,γ-dihydroxyl substitution pattern. In the HSQC spectrum, peaks can be assigned to the α, β, γ_1, and γ_2 positions in monomer A (Figure 7), but no peaks can be assigned to the side chain of monomer B. Peaks can also be assigned to the α and β positions of monomer C (Figures 7 and 8). In the TOCSY spectrum, peaks are present that could correlate the α, β, and γ hydrogens of monomer A as well as those of monomer B (Figure 13). However, there are no TOCSY peaks that correlate the side chain Hs of monomer C, so it is unlikely that the free side chain of monomer C is present in the biodegraded wood sample. While the evidence supports the presence of the isochroman structure, the HSQC and TOCSY peaks assigned to the side chains involved in the linkage are also assigned to other lignin structures.

The spirodienone structure in compound XIII involves the side chains of both the A and B monomers. HSQC peaks can be assigned to Aγ_1, Aγ_2, Bα, Bγ_1, and Bγ_2 (Figure 7). There is not strong evidence for the structure, however, even though peaks in the TOCSY spectrum could correlate the α, β, γ_1, and γ_2 hydrogens of monomer A as well as those of monomer B (Figures 10 and 13); with the exception of two small, slightly misaligned peaks in the TOCSY spectrum, all of the NMR peaks indicating the presence of the spirodienone structure can also be assigned to other side chains.

HSQC and TOCSY peaks could not be assigned to some of the Cs and Hs of compounds I through XIII. The dimer/trimer compounds utilized in this study serve the purpose of modeling the types of polymeric units that likely exist in the biodegraded BR-lignin, and as such, a missing cross peak in the spectrum may not necessarily mean the absence of that type of structure in the BR-lignin sample. Some cross peaks found in the TOCSY spectrum are particularly strong and diagnostic, such as the peaks formed from a side chain consisting of an aldehyde attached to an alkene, and no peaks corresponding to that side chain are present in the HSQC spectrum. An HSQC spectrum was acquired using larger spectral widths in both the ^{1}H and ^{13}C dimensions to search for aldehyde signals, but only 64 scans were acquired in the ^{1}H dimension. No aldehyde signals were observed in this broadened spectral data set, but a longer data acquisition time may have produced the missing aldehyde peaks.

CONCLUSIONS

In summary, because lignin is a major component of wood, as well as a likely precursor to soil organic matter, there is a need for its accurate molecular characterization. Here, the HRMAS technique for swelled solids has made it

possible to obtain highly resolved 2D NMR spectra of biodegraded, brown-rotted (BR) lignin with little alteration other than hand grinding (with a mortar and pestle) and the addition of DMSO-d_6. The HSQC and TOCSY spectra obtained provide an accurate representation of lignin from this biodegraded wood. It is clear from the CPMAS ^{13}C NMR spectrum of the biodegraded BR-lignin that the sample has lost most of its carbohydrates. This is consistent with the fact that the BR fungi acting on it have selectively utilized the polysaccharides from the wood, and the residual wood is mainly lignin. The HSQC spectrum is also consistent with this. The presence of signals for polymethylenic structures in the CPMAS, HSQC, and TOCSY spectra suggest that residual lipids could be present, most likely from the microbial degradation.

This study, employing a noninvasive approach, supports the existence of several of the major types of lignin linkages (Figure 2). The NMR spectra suggest that the β-1 linkage may not be present in this biodegraded BR-lignin. Evidence for the dibenzodioxocin structure is clear, and further support for the isochroman structure is presented (Figure 3). The evidence for the presence of spirodienones is weak. The HSQC and TOCSY spectra were analyzed for the presence of side chains at a range of oxidation states. Peaks can be assigned to side chains showing varying levels of O-substitution in the biodegraded BR-lignin (Figures 2 and 3). Many of the types of side chains analyzed in this study have previously been found in extracted lignins. However, to our knowledge, over half of them have not. This study cannot, however, serve as a final confirmation of the presence of many of the analyzed partially-hydroxylated side chains, because the sample may contain lipids that could be mistaken for these types of lignin structures.

The HSQC and TOCSY HRMAS NMR spectra of biodegraded BR-lignin corroborate the current basic understanding of the lignin structure. The spectra support the existence of several linkages in this residual lignin that have commonly been accepted as being present in extracted lignins and ball-milled cell walls from fresh wood and model compounds. It is difficult to determine the extent of microbial modification to this BR-lignin, because methoxylated aromatics produce cross peaks at similar chemical shifts as their hydroxylated derivatives, and an increase in oxidized side chains cannot be easily measured with these NMR techniques. Comparison of non-degraded wood with this sample would seem to be a logical extension of this work, but some significant consideration for the influence of cellulosic components on the HRMAS spectra would need to be made, and this is beyond the scope of this article.

REFERENCES

1. Monties, B.; Fukushima, K. Occurrence, function and biosynthesis of lignins. In *Biopolymers, Volume 1: Lignin, Humic Substances and Coal*; Hofrichter, M., Steinbüchel, A., Eds.; Wiley-VCH; Weinheim, 2001; 1–64.

2. Lai, Y.-Z.; Funaoka, M.; Chen, H.-T. Chemical heterogeneity in wood lignins. In *Advances in Lignocellulosics Characterization*; Argyropoulos, D.S., Ed.; Tappi Press; Atlanta, 1999; 43–53.
3. Stevenson, F.J. *Humus Chemistry: Genesis, Composition, Reactions, 2nd Edition*; John Wiley & Sons, Inc.: New York, NY, 1994; 188–211.
4. Ralph, J.; Marita, J.M.; Ralph, S.A.; Hatfield, R.D.; Lu, F.; Ede, R.M.; Peng, J.; Quideau, S.; Helm, R.F.; Grabber, J.H.; Kim, H.; Jimenez-Monteon, G.; Zhang, Y.; Jung, H.-J.G.; Landucci, L.L.; MacKay, J.J.; Sederoff, R.R.; Chapple, C.; Boudet, A.M. Solution-state NMR of lignins. In *Advances in Lignocellulosics Characterization*; Argyropoulos, D.S., Ed.; Tappi Press; Atlanta, 1999; 55–108.
5. Zhang, L.; Henriksson, G.; Gellerstedt, G. The formation of β-β structures in lignin biosynthesis—Are there two different pathways? Org. Biomol. Chem., **2003**, *1* (20), 3621–3624.
6. Zhang, L.; Gellerstedt, G.; Ralph, J.; Lu, F. NMR studies on the occurrence of spirodienone structures in lignin. J. Wood Chem. Technol. **2006**, *26* (1), 65–79.
7. Holtman, K.M.; Chang, H-M.; Kadla, J.F. An NMR comparison of the whole lignin from milled wood, MWL, and REL dissolved by the DMSO/NMI procedure. J. Wood Chem. Technol. **2007**, *27* (3-4), 179–200.
8. Kim, H.; Ralph, J.; Akiyama, T. Solution-state 2D NMR of ball-milled plant cell wall gels in DMSO-d_6. Bioener. Res. **2008**, *1* (1), 56–66.
9. Yelle, D.J.; Ralph, J.; Frihart, C.R. Characterization of nonderivatized plant cell walls using high-resolution solution-state NMR spectroscopy. Magn. Reson. Chem. **2008**, *46* (6), 508–517.
10. Capanema, E.A.; Balakshin, M.Y.; Kadla, J.F. Quantitative characterization of a hardwood milled wood lignin by nuclear magnetic resonance spectroscopy. J. Agr. Food Chem. **2005**, *52* (25), 9639–9649.
11. Lundquist, K. Wood. In *Methods in Lignin Chemistry*; Lin, S.Y., Dence, C.W., Eds.; Springer-Verlag; Berlin, 1992; 65–70.
12. Adler, E. Lignin chemistry—Past, present, and future. Wood Sci. Technol. **1977**, *11* (3), 169–218.
13. Hatcher, P.G.; Wilson, M.A.; Vassallo, A.M.; Lerch III, H.E. Studies of angiospermous wood in Australian brown coal by nuclear magnetic resonance and analytical pyrolysis: New insights into the early coalification process. Int. J. Coal Geol. **1989**, *13* (1–4), 99–126.
14. Gil, A.M.; Neto, C.P. Solid-state NMR studies of wood and other lignocellulosic materials. Ann. R. NMR S. **1999**, *37*, 75–117.
15. Ralph, J.; Peng, J.; Lu, F. Isochroman structures in lignin: A new β-1 pathway. Tetrahedron Lett. **1998**, *39* (28), 4963–4964.
16. Landucci, L.L.; Ralph, S.A.; Hammel, K.E. ^{13}C NMR characterization of guaiacyl, guaiacyl/syringyl, and syringyl dehydrogenation polymers. Holzforschung. **1998**, *52* (2), 160–170.
17. Ralph, J.; Lundquist, K.; Brunow, G.; Lu, F.; Kim, H.; Schatz, P.F.; Marita, J.M.; Hatfield, R.D.; Ralph, S.A.; Christensen, J.H.; Boerjan, W. Lignins: Natural polymers from oxidative coupling of 4-hydroxyphenylpropanoids. Phytochemistry Rev. **2004a**, *3* (1–2), 29–60.
18. Bartuska, V.J.; Maciel, G.E. Structural studies of lignin isolation procedures by ^{13}C NMR. Holzforschung. **1980**, *34* (6), 214–217.

19. Maciel, G.E.; O'Donnell, D.J.; Ackerman, J.J.H.; Hawkins, B.H.; Bartuska, V.J. A carbon-13 NMR study of four lignins in the solid and solution states. Makromol. Chem. **1981**, *182* (8), 2297–2304.
20. Keifer, P.A.; Baltusis, L.; Rice, D.M.; Tymiak, A.A.; Shoolery, J.N. A comparison of NMR spectra obtained for solid-phase-synthesis resins using conventional high-resolution, magic-angle-spinning, and high-resolution magic-angle-spinning probes. J. Magn. Reson. Ser. A. **1996**, *119* (1), 65–75.
21. Millis, K.K.; Maas, W.E.; Cory, D.G.; Singer, S. Gradient, high-resolution, magic-angle spinning nuclear magnetic resonance spectroscopy of human adipocyte tissue. Magnet. Reson. Med. **1997**, *38* (3), 399–403.
22. Power, W.P. High resolution magic angle spinning—Applications to solid phase synthetic systems and other semi-solids. Ann. R. NMR S. **2003**, *51*, 261–295.
23. Simpson, A.J.; Zang, X.; Kramer, R.; Hatcher, P.G. New insights on the structure of algaenan from *Botryoccocus braunii* race A and its hexane insoluble botryals based on multidimensional NMR spectroscopy and electrospray-mass spectrometry techniques. Phytochemistry. **2003**, *62* (5), 783–796.
24. Kelleher, B.P.; Simpson, M.J.; Simpson, A.J. Assessing the fate and transformation of plant residues in the terrestrial environment using HR-MAS NMR spectroscopy. Geochim. Cosmochim. Ac. **2006**, *70* (16), 4080–4094.
25. Deshmukh, A.P.; Simpson, A.J.; Hatcher, P.G. Evidence for cross-linking in tomato cutin using HR-MAS NMR spectroscopy. Phytochemistry. **2003**, *64* (6), 1163–1170.
26. Deshmukh, A.P.; Simpson, A.J.; Hadad, C.M.; Hatcher, P.G. Insights into the structure of cutin and cutan from *Agave americana* leaf cuticle using HRMAS NMR spectroscopy. Org. Geochem. **2005**, *36* (7), 1072–1085.
27. Salmon, E.; Behar, F.; Lorant, F.; Hatcher, P.G.; Metzger, P.; Marquaire, P.-M. Thermal decomposition processes in algaenan of *Botryococcus braunii* race L. Part 1: Experimental data and structural evolution. Org. Geochem. **2009**, *40* (3), 400–415.
28. Salmon, E.; Behar, F.; Lorant, F.; Hatcher, P.G.; Marquaire, P.-M. Early maturation processes in coal. Part 1: Pyrolysis mass balance and structural evolution of coalified wood from the Morwell Brown Coal seam. Org. Geochem. **2009**, *40* (4), 500–509.
29. Hatcher, P.G. Chemical structural studies of natural lignin by dipolar dephasing solid-state ^{13}C nuclear magnetic resonance. Org. Geochem. **1987**, *11* (1), 31–39.
30. Hatcher, P.G. Dipolar-dephasing ^{13}C NMR studies of decomposed wood and coalified xylem tissue: evidence for chemical structural changes associated with defunctionalization of lignin structural units during coalification. Energ. Fuel. **1988**, *2* (1), 48–58.
31. Blanchette, R.A.; Obst, J.R.; Timell, T.E. Biodegradation of compression wood and tension wood by white and brown rot fungi. Holzforschung. **1994**, *48* (suppl), 34–42.
32. Dria, K.J.; Sachleben, J.R.; Hatcher, P.G. Solid-state carbon-13 nuclear magnetic resonance of humic acids at high magnetic field strengths. J. Environ. Qual. **2002**, *31* (2), 393–401.
33. Ralph, S.A.; Ralph, J.; Landucci, L.L. NMR database of lignin and cell wall model compounds. 2004b, Available at http://ars.usda.gov/Services/docs.htm?docid=10491

34. Kishimoto, T.; Uraki, Y.; Ubukata, M. Synthesis of b-O-4-type artificial lignin polymers and their analysis by NMR spectroscopy. Org. Biomol. Chem. **2008**, *6* (16), 2982–2987.
35. Brunow, G.; Ammalahti, E.; Niemi, T.; Sipila, J.; Simola, L.K.; Kilpelainen, I. Labeling of a lignin from suspension cultures of *Picea abies*. Phytochemistry **1998a**, *47* (8), 1495–1500.
36. Boerjan, W.; Ralph, J.; Baucher, M. Lignin biosynthesis. Ann. Rev. Plant Biol. **2003**, *54*, 519–546.
37. Karhunen, P.; Rummakko, P.; Sipilä, J.; Brunow, G.: Dibenzodioxocins; a novel type of linkage in softwood lignins. Tetrahedron Lett. **1995a**, *36* (1), 169–170.
38. Karhunen, P.; Rummakko, P.; Sipilä, J.; Brunow, G. The formation of dibenzodioxocin structures by oxidative coupling. A model reaction for lignin biosynthesis. Tetrahedron Lett. **1995b**, *36* (25), 4501–4504.
39. Brunow, G.; Kilpeläinen, I.; Sipilä, J.; Syrjänen, K.; Karhunen, P.; Setälä, H.; Rummakko, P. Oxidative coupling of phenols and the biosynthesis of lignin. In *Lignin and Lignan Biosynthesis*; Lewis, N.G., Sarkanen, S., Eds.; ACS Symposium Series 697, American Chemical Society; Washington, D.C., 1998b; 131–147.
40. Peng, J.; Lu, F.; Ralph, J. Isochroman lignin trimers from DFRC-degraded *Pinus taeda*. Phytochemistry. **1999**, *50* (4), 659–666.
41. Fagerstedt, K.V. The dibenzodioxocin lignin substructure is abundant in the inner part of the secondary wall in Norway spruce and silver birch xylem. Planta. **2004**, *218* (3), 497–500.
42. Argyropoulos, D.S.; Jurasek, L.; Kristofova, L.; Xia, Z.; Sun, Y.; Palus, E. Abundance and reactivity of dibenzodioxocins in softwood lignin. J. Agr. Food Chem. **2002**, *50* (4), 658–666.
43. Zhang, L.; Gellerstedt, G. NMR Observations of a new lignin structure, a spirodienone. Chem. Commun. **2001**, (24), 2744–2745.
44. Filley, T.R.; Cody, G.D.; Goodell, B.; Jellison, J.; Noser, C.; Ostrofsky, A. Lignin demethylation and polysaccharide decomposition in spruce sapwood degraded by brown rot fungi. Org. Geochem. **2002**, *33* (2), 111–124.
45. Martínez, A.T.; Almendros, G.; González-Vila, F.J.; Fründ, R. Solid-state spectroscopic analysis of lignins from several Austral hardwoods. Solid State Nucl. Mag. **1999**, *15* (1), 41–48.
46. Bates, A.L.; Hatcher, P.G.; Lerch III, H.E.; Cecil, C.B.; Neuzil, S.G.; Supardi. Studies of a peatified angiosperm log cross section from Indonesia by nuclear magnetic resonance spectroscopy and analytical pyrolysis. Org. Geochem. **1991**, *17* (1), 37–45.
47. Earl, W.L.; VanderHart, D.L. High resolution, magic angle sample spinning ^{13}C NMR of solid cellulose I. J. Am. Chem. Soc. **1980**, *102* (9), 3251–3252.
48. Ralph, J.; Akiyama, T.; Kim, H.; Lu, F.; Schatz, P.F.; Marita, J.M.; Ralph, S.A.; Reddy, M.S.S.; Chen, F.; Dixon, R.A. Effects of coumarate 3-hydroxylase down-regulation on lignin structure. J. Biol. Chem. **2006**, *281* (13), 8843–8853.